Astronomy in Focus, Volume 1, Focus Meeting 12
XXIXth IAU General Assembly, August 2015
Piero Benvenuti, ed.

doi:10.1017/S1743921316003239

Recent Status of Multi-Dimensional Core-Collapse Supernova Models

Kei Kotake[1] , Ko Nakamura[2] and Tomoya Takiwaki[3]

[1]Department of Applied Physics, Fukuoka University, Jonan, Nanakuma, Fukuoka 814-0180, Japan

[2]Faculty of Science and Engineering, Waseda University, Ohkubo 3-4-1, Shinjuku, Tokyo 169-8555

[3]Astrophysical Big Bang Laboratory, RIKEN, Saitama, 351-0198, Japan

Abstract. We report a recent status of multi-dimensional neutrino-radiation hydrodynamics simulations for clarifying the explosion mechanism of core-collapse supernovae (CCSNe). In this contribution, we present two results, one from two-dimensional (2D) simulations using multiple progenitor models and another from three-dimensional (3D) rotational core-collapse simulation using a single progenitor. From the first ever systematic 2D simulations, it is shown that the compactness parameter ξ that characterizes the structure of the progenitors is a key to diagnose the explodability of neutrino-driven explosions. In the 3D rotating model, we find a new type of rotation-assisted explosion, which makes the explosion energy bigger than that in the non-rotating model. The unique feature has not been captured in previous 2D self-consistent rotational models because the growth of *non-axisymmetric* instabilities is the key to foster the explosion by enhancing the energy transport from the proto-neutron star to the gain region.

Keywords. Hydrodynamics—Neutrinos—Supernovae: general

1. Introduction

Core-collapse supernova (CCSN) mechanism is essentially an initial value problem. For low-mass progenitors with O-Ne-Mg core, the neutrino mechanism works successfully to explode in one-dimensional (1D) simulations because of the tenuous envelope (Kitaura et al.(2006)). For more massive progenitors with iron core, multi-dimensional (multi-D) effects such as neutrino-driven convection and the standing-accretion-shock-instability (SASI) have been suggested to help the onset of the neutrino-driven explosion. Recently this has been confirmed by a number of self-consistent two-(2D) and three-dimensional (3D) simulations (see collective references in Mezzacappa *et al.*(2015), Foglizzo *et al.*(2015), Janka(2012), Kotake *et al.*(2012)). Up to now, the number of these state-of-the-art models amounts to $\sim$ 40 covering the zero-age main sequence (ZAMS) mass from 8.1 $M_\odot$ to 27 $M_\odot$ (Hanke *et al.* (2013)).

In this contribution, we first summarize our recent results (Nakamura *et al.*(2015)), in which we have computed first ever systematic 2D neutrino radiation hydrodynamics simulations using the whole progenitors (i.e., 378 models in total including 101 solar-metallicity models, 247 ultra metal-poor models, and 30 zero-metal models) in Woosley *et al.* (2002). By following a long-term evolution over 1.0 s after bounce, we have shown that most of the computed models exhibit neutrino-driven revival of the stalled bounce shock at $\sim$ 200 - 800 ms postbounce, leading to the possibility of explosions.

This success, however, is now raising new questions. With the exception in Bruenn *et al.* (2013), the explosion energies obtained in these 2D models are typically smaller by one order of magnitude in explaining the canonical supernova kinetic energy of 10^{51} erg

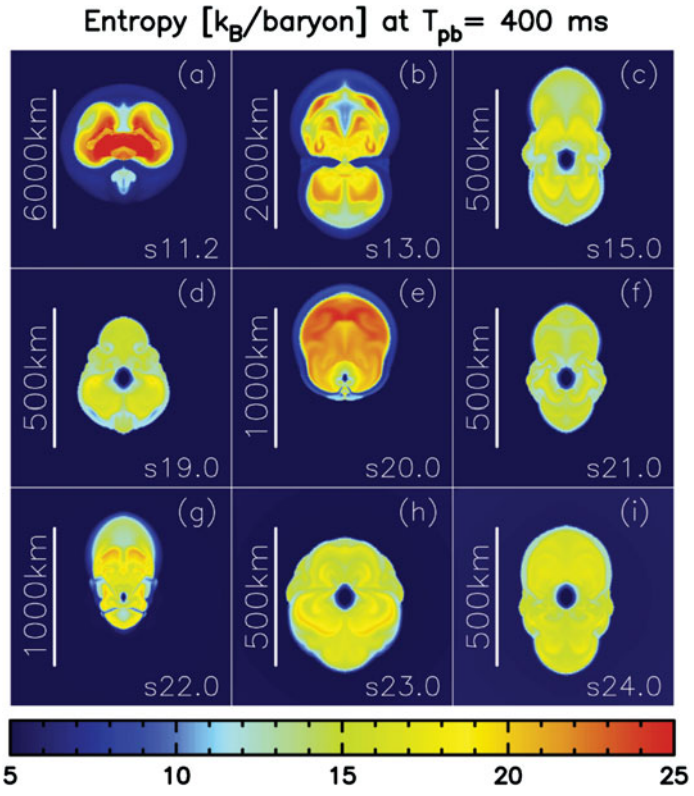

Figure 1. 2D Blast morphologies for multiple progenitor models with different masses from 11.2 (top left panel) to 24 $M_\odot$ (bottom left panel). Shown are entropy distributions in unit of $k_{\rm B}$ per baryon at $t_{\rm pb} = 400$ ms after bounce. Note that each model presents a different scale as shown in the panel.

(Tanaka *et al.* (2009)). Most researchers are now seeking for some ingredients to make these underpowered explosions more energetic. In the latter half of this contribution, we report our most up-to-date results based on 3D rotational core-collapse simulations and discuss effects of stellar rotation on fostering the onset of neutrino-driven explosions (Takiwaki, Kotake, Suwa (2015)).

2. 2D Systematic Simulations Using Multiple Progenitors

In all of the computed models, the bounce shock stalls in a spherically symmetric manner and only after that, we observe a clear diversity of the multi-D hydrodynamics evolution in the postbounce (pb) phase. Figure 1 shows a snapshot of entropy distribution for selected nine solar-metallicity models at $t_{\rm pb} = 400$ ms. For some less massive progenitors (e.g., s11.2 (panel (a))) the shock is reaching close to the outer boundary of the computational domain with developing pronounced unipolar and dipolar shock deformations. At this time, the shock of the most massive progenitor (s75.0) is reaching an average radius of $\langle r \rangle \sim 1000$ km, whereas the shock of s24.0 (panel (i)) still wobbles around at $\langle r \rangle \sim 200$ km. This demonstrates that the progenitor mass is not a good criterion to diagnose the possibility of explosion.

This is more clearly visualized in the left panel of Figure 2, showing time evolution of average shock radii for six models in the mass range between 19.0 $M_\odot$ and 24.0 $M_\odot$. The

https://doi.org/10.1017/S1743921316003239 Published online by Cambridge University Press

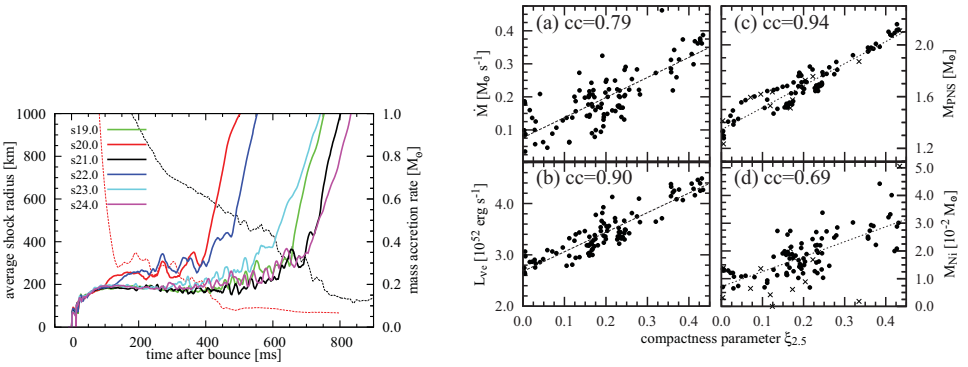

Figure 2. Left panel shows average shock radii (thick solid lines) and mass-accretion rate of the collapsing stellar core at 500 km (thin dashed lines) for some selected models (solar metallicity). Right panel summarizes explodability diagnostics versus the compactness parameter $\xi_{2.5}$ for the 101 solar-metallicity models (see Nakamura *et al.*(2015) for details about the rest of the progenitor series). Panel (a) is the mass accretion rate $\dot{M}$, panel (b) electron neutrino luminosity $L_{\nu e}$ estimated both at time of shock revival t_{400}, panel (c) is the mass of proto-neutron star (PNS) $M_{\rm PNS}$, and (d) mass of nickel $M_{\rm Ni}$ in outgoing unbound material at final time of our simulations $t_{\rm fin}$. Dashed lines present linear fitting with correlation coefficient denoted in each panel.

shock revival is shown to occur earlier for s20.0 (red line) and s22.0 (blue line) compared to the lighter progenitors s19.0 (green line) and s21.0 (black line). The progenitor compactness parameter ξ† is smaller for s20.0 and s22.0 in the chosen mass range. The smaller compactness is translated into smaller mass accretion rate onto the stalled bounce shock. For model s20.0 the relatively earlier shock revival coincides with the sharp decline of the accretion rate (dashed red line). After that, the accretion rate gradually decreases to $\sim 0.1\ M_\odot\,{\rm s}^{-1}$ till $t_{400} = 420$ ms at this time the revived shock has expanded to an average radius of $\langle r\rangle = 400$ km. Here t_{400} is a useful measure to qualify the vigour of the shock revival. On the other hand, model s21.0 has high compactness, which leads to the high accretion rate (black dashed line). It takes ~ 500 ms for the sloshing shock of model s21.0 (black solid line) to gradually turn into a pronounced expansion later on and 700 ms to arrive at $\langle r\rangle = 400$ km ($t_{400} = 700$ ms).

To summarize the explodability of the multiple progenitor models, we show in the right panel of Figure 2 various diagnostic properties as a function of the compactness parameter ($\xi_{2.5}$). Pushing the boundaries of expectations in previous 1D studies (e.g., Ugliano *et al.* (2012)), our results confirm that the compactness parameter ξ that characterizes the structure of the progenitors is also a key in 2D to diagnose the properties of neutrino-driven explosions. These results can be interpreted as follows: the core of high-ξ models is surrounded by high-density Si/O layers and the mass accretion rate therefore remains high long after the stalled shock has formed. This makes the PNS mass of the high-ξ models heavier (panel (c)). Due to the high accretion rate (panel (a)), the accretion neutrino luminosities become higher for models with high ξ (panel (b)). As a result, a stronger shock revival is obtained due to the more intense neutrino heating, which makes the amount of the synthesized nickel bigger (panel (d)). Our 2D simulations are terminated before the diagnostic (explosion) energies are saturated. However, a simple estimation regarding the mass accretion rate and the time derivative of the diagnostic

† Following O'Connor & Ott(2011), we define it as the ratio of mass M and the enclosed radius $R(M)$, $\xi_{2.5} \equiv \frac{M/M_\odot}{R(M=2.5\ M_\odot)/1000{\rm km}}$.

https://doi.org/10.1017/S1743921316003239 Published online by Cambridge University Press

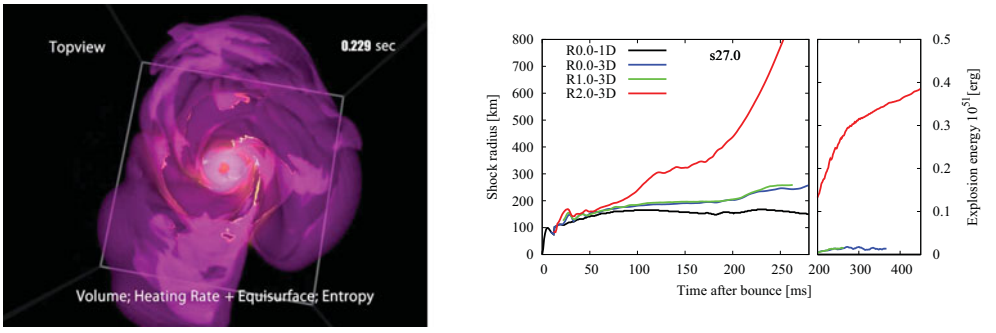

Figure 3. 3D image (left panel) shows a snapshot (at 229 ms after bounce) of the 3D rotating model ($\Omega_0 = 2$ rad/s, 27 $M_\odot$ star (Woosley *et al.* (2002))) seen from the direction parallel to the spin axis. Due to the growth of non-axisymmetric instabilities, the explosion develops preferentially toward the equatorial direction. Right panel shows the evolution of the (average) shock radii and the diagnostic explosion energy for the 1D or 3D models without rotation or with rotation, with R0.0, R1.0, and R2.0 representing $\Omega_0 = 0$ (non-rotating), 1, and 2 rad/s, respectively.

explosion energy may suggest that the diagnostic energy could barely reach 10^{51} erg ($\equiv 1$ Bethe) in most of the 2D models. It is true that further global simulation, taking account of gravitational energy of an envelope and nuclear energy released via recombination process behind the shock, is necessary to determine the final explosion energy, but there might be some missing ingredients in 2D models to account for the 1 Bethe.

3. Seeking Ingredients to Foster Explosions : Impacts of Rotation

Here we focus on the roles of rotation and report results from a series of 3D rotational core-collapse simulations with spectral neutrino transport for a $27M_\odot$ star. The initially constant angular frequency of $\Omega_0 = 1$ or 2 rad/s is imposed inside the iron core with a cut-off ($\propto r^{-2}$) outside. We assume such rapid rotation to clearly see the impacts of rotation in this study.

As depicted in the left panel of Figure 3, we find a new type of rotation-assisted explosion for the $27M_\odot$ model, which otherwise fails to work when the precollapse core has no angular momentum (right panel of Figure 3). The unique feature was not captured in previous 2D self-consistent rotational models (e.g., Suwa *et al.*(2010)) because the growth of *non-axisymmetric* instabilities is the key to foster the explosion by enhancing the energy transport from the PNS to the gain region (see Takiwaki, Kotake, Suwa (2015) for more details). By systematically changing the precollapse rotation rates, we furthermore point out that rotation has also negative effects on the shock-revival, which was not treated accurately in previous 3D rotating models with fixed core neutrino luminosity or excision inside the PNS (e.g., Nakamura *et al.*(2014)). The SASI-modulated neutrino emission is significantly affected by the inclusion of rotation and the interesting correlation with the gravitational-wave emission is also found. Detailed coherent detector network analysis (e.g., Hayama *et al.*(2015)) of the correlated signals will be submitted elsewhere very soon.

References

Kitaura, F. S., Janka, H.-T., & Hillebrandt, W. 2006, A&A, 450, 345
Mezzacappa, A., Bruenn, S. W., Lentz, E. J., *et al.* 2015, arXiv:1501.01688

https://doi.org/10.1017/S1743921316003239 Published online by Cambridge University Press

Foglizzo, T., Kazeroni, R., Guilet, J., *et al.* 2015, arXiv:1501.01334
Janka, H.-T., 2012, *Annual Review of Nuclear and Particle Science*, 62, 407
Kotake, K., Sumiyoshi, K., Yamada, S., *et al.* 2012, Progress of Theoretical and Experimental Physics, 2012, 01A301
Hanke, F., Müller, B., Wongwathanarat, A., Marek, A., & Janka, H.-T. 2013, *ApJ*, 770, 66
Nakamura, K., Takiwaki, T., Kuroda, T., & Kotake, K. 2014, arXiv:1406.2415, accepted to PASJ
Woosley, S. E., Heger, A., & Weaver, T. A. 2002, *Reviews of Modern Physics*, 74, 1015
Bruenn, S. W., Mezzacappa, A., Hix, W. R., *et al.* 2013, ApJL, 767, L6
Tanaka, M., Kawabata, K. S., Maeda, K., *et al.* 2009, *ApJ*, 699, 1119
Takiwaki, T., Kotake, K., Suwa, Y, in preparation
O'Connor, E. & Ott, C. D. 2011, *ApJ*, 730, 70
Ugliano, M., Janka, H.-T., Marek, A., & Arcones, A. 2012, *ApJ*, 757, 69
Suwa, Y., Kotake, K., Takiwaki, T., *et al.* 2010, PASJ, 62, L49
Nakamura, K., Kuroda, T., Takiwaki, T., & Kotake, K. 2014, *ApJ*, 793, 45
Hayama, K., Kuroda, T., Kotake, K., & Takiwaki, T. 2015, arXiv:1501.00966